

A SIMULATION FRAMEWORK FOR PHOTON-PARTICLE INTERACTIONS FOR LASERWIRES AND FURTHER APPLICATIONS

S. E. Alden*, S. M. Gibson, L. J. Nevay, JAI at Royal Holloway University of London, Egham, UK

Abstract

A model has been developed for simulating photon-particle interactions with Beam Delivery Simulation (BDSIM). BDSIM is a high energy physics program that utilises the Geant4, CLHEP, and ROOT libraries to seamlessly track particles through an accelerator. The photon-particle interactions introduce the capability for modelling a range of applications in accelerator physics. One such application is a laserwire which is a minimally invasive diagnostic technique to measure beam profiles and emittance. In this paper we describe the recent implementation of inverse Compton scattering and electron stripping of Hydrogen ions. This is demonstrated in an example beamline.

INTRODUCTION

A laserwire provides a non-invasive diagnostic method to measure beam profiles and emittance for electron, positron, and hydrogen ion beams. For both cases the basic configuration [1] is as shown in Fig. 1. A tightly focused laser pulse crosses the particle beam, resulting in particle-photon interactions. By carefully calibrating the laser, the interaction rate arising from this method is sufficient for characterising the particle bunch. The majority of the beam continues unperturbed and can be redirected.

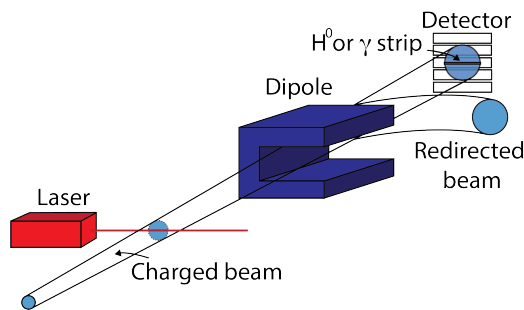


Figure 1: Typical layout for a diagnostic laserwire.

In the case of a H^- ion, the weakly bound second electron can easily undergo photodetachment with an optical wavelength photon. The free electrons can be measured with detectors such as a Faraday cup, which combined with multiple measurements of varying transverse laserwire offsets across the ion beam builds a profile. Alternatively the remaining H^- can be redirected via dipole leaving the H^0 to drift to a detector. This method allows both the beam profile and beam emittance to be measured. The angular divergence of the beam is evaluated by the difference between the spatial signal at the detector plane relative to the laserwire transverse placement and the drift distance between the

two [2]. Examples of laserwire diagnostics for hydrogen ion beams have been demonstrated at SNS [3] and LINAC4 at CERN [4, 5].

In the case of electron beams the laserwire is based on inverse Compton scattering of the photons from the incident electrons or positrons. The high energy photons are scattered along the direction of the particle beam and can be detected after the charged particles are typically separated using a dipole magnet. A profile is constructed from measuring the modulated rate of scattered photons as the laser beam is transversely scanned across the particle beam. In some cases the scattered electrons can also be detected, for example in very high energy e^- beams, where the electron kinetic energy can be reduced by up to half the original value. Examples of laserwire beam profile monitors for electron beams have been demonstrated at the ATF2 at KEK [6], and PETRA II at DESY [7].

BEAM DELIVERY SIMULATION

BDSIM is a program that uses high energy physics software including Geant4, CLHEP, and ROOT, to construct a 3D model of an accelerator [8]. The particles are then tracked through the magnetic lattice using BDSIM's thick lens accelerator tracking in a vacuum. The model is constructed from a range of generic of accelerator components including magnets. GEANT4 physics processes are used to simulate interactions between the particles and the medium through which a particle is travelling. A single particle is tracked until kinetic energy reaches zero or it leaves the world according to the physics processes in the model. Any secondary particles are also tracked similarly.

MODEL APPROACH

To provide both photodetachment and inverse-Compton scattering particle-photon interactions two processes were added to Geant4. The model approach for both processes are the same but apply to different charged beams and provide different outcomes. A geometric model of a laserwire is constructed as a hyperboloid, as seen in Fig. 2. The hyperbolic angle is defined as $\theta = \frac{M^2 \lambda}{\pi w_0}$, where M^2 is the beam quality, λ is the laser wavelength, and w_0 is the laser waist. The minimum radius is constructed at $10\sigma_l$, the laser beam size, or $5w_0$.

For uniform density media the variation in intensity of incident particles through a medium are described by the Beer-Lambert law. This can be used to define a mean free path based upon density of the material that is being traversed. In the case of the laser, the photon density is non-uniform. An alternative approach is to define a probability of interaction

* siobhan.alden.2014@live.rhul.ac.uk

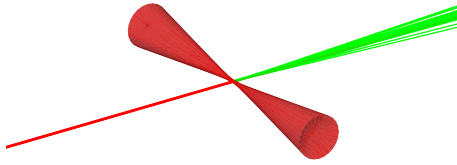


Figure 2: Laserwire Geometry with Compton Scatter process with a laser wavelength of 532 nm where the incoming, and scattered electrons are in red, and the scattered photons in green.

with the laserwire photons for the path of particle [9]. The probability is characterised by

$$P_s = 1 - \exp^{-\sigma(\lambda)\rho(x,y,z)t} \quad (1)$$

where $\sigma(\lambda)$ is the interaction cross section as a function of the laser wavelength, λ , $\rho(x, y, z)$ is the photon flux of the laserwire, $I(r, z)$, divided by the photon energy, E_γ , and t is the integrated time. The photon flux is modelled using Gaussian beam optics and is characterised by

$$I(r, z) = \frac{2P}{\pi w(z)^2} \exp\left(\frac{-2r^2}{w(z)^2}\right) \quad (2)$$

where P is the peak power of the laser, defined as the pulse energy divided by the pulse duration, r is the radius in relation to the laser axis, and $w(z)$ is the laser width based upon the displacement, z , from the laser focus. The laser width, $w(z) = w_0 \sqrt{1 + \left(\frac{z}{z_R}\right)^2}$ is dependant on the laser waist, and z_R is the Rayleigh distance. As seen in Equation 2, the spatial dependence of photon flux experienced along the path of the particle through the laser beam is also non-uniform. As a result of the non-uniformity, previous simulations [10] have modelled the non-uniform flux by gradually calculating a cumulative probability from the sum of discrete steps, as illustrated in Fig. 3. Equation 2 describes a static pulse that applies in the case where the laser pulse duration is much longer than the bunch. In the case where the laser pulse duration is of the same order as the ion bunch duration the photon flux is modified by the laser temporal profile.

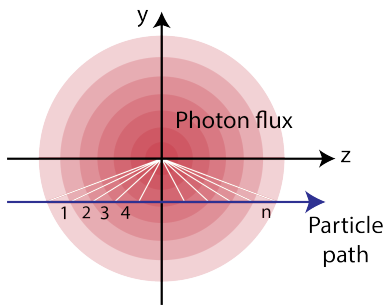


Figure 3: Schematic of laser photon flux experienced by a particle transiting the laser beam transversely.

To simulate the probability of interaction in BDSIM the path of each particle inside the laser volume is discretised by proposing a mean free path of $\frac{\sigma_l}{10}$ and forcing the interaction condition. The $10\sigma_l$ radial limit on the geometry is chosen as the photon flux at a radius greater than $10\sigma_l$ yields a negligible probability of interaction. The probability of interaction for each step is then calculated using Equation 1 and the time taken between the current and previous step coordinates, taking into account the particle velocity. This probability is then compared to a random number, if it is the greater of the two the particle interaction is triggered. Due to the low interaction rate for both processes a scale factor can be specified with is applied linearly to the probability of interaction.

For the photodetachment model the interaction generates a secondary electron particle and neutralises the incoming H^- ion. The secondary electron in the H^- ion has a binding energy of only 0.75 eV. The photo-neutralization cross-section is calculated from Broad and Reinhardt [11] along with the Doppler shifted photon energy. The outgoing electron kinematics are defined by the primary H^- ion. For Compton Scattering the secondary particle is a photon that is produced using the Klein-Nishina cross-section [12]. The scattered photon energy is calculated based on the laser photon energy, the species of particle from which the photon has scattered, and a randomly generated angle in the rest frame of the beam particle.

SIMULATION STUDIES

The Compton scattering from electrons, and H- photo-detachment processes were both modelled using the laser and relevant beam parameters in Table 1. The model was arranged with the laser orthogonal to the particle beam axis. For the electron beam, a million particles were generated with a scale factor of 100 applied to the probability of interaction. For the initial H^- beam 10 million primary particles were generated with a scale factor of 10. Both processes have a low interaction rate so the scale factor is applied to increase secondary particle statistics.

Table 1: Simulated Electron and Laser Beam Parameters for Interaction

Parameter	e ⁻ value	H ⁻ value
Laser pulse energy (E_l)	150 mJ	67.5 μ J
Wavelength (λ)	532 nm	1064 nm
Laser pulse duration (P_l)	70.8 ps	106 ns
σ_l	1 μ m	5 μ m
M^2	1.8	1.8
Electron Beam Energy	1.3 GeV	6 MeV
σ_{ex}	50 μ m	-
σ_{ey}	100 μ m	-
ϵ_x	-	5.9 mm mrad
ϵ_y	-	5.6 mm mrad
Scale factor laser	100	10

In the case of the inverse Compton scattering process, the scattered photons were recorded 5 cm downstream of the laser, transversely across the full beam pipe. The total yield of scattered photons was 14% of the primary generated electrons. Plotting the energy spectrum of the scattered photons reveals a distribution characteristic of Compton scattering, seen in Fig. 4.

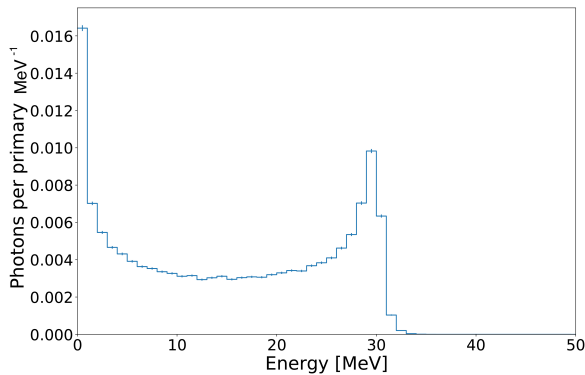


Figure 4: Energy spectrum of Compton scattered photons.

For the photodetachment process the ejected electrons were also measured 5 cm downstream of the laser, transversely across the full beam pipe. The the transverse distribution of ejected electrons can seen in Fig. 5. This distribution reveals the hyperbolic profile of the laser from the convolution of the ion beam and the laser in the resultant electrons. The area of highest density of electrons is found at the laser waist.

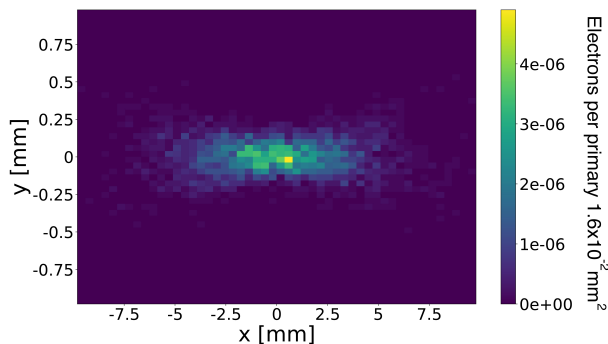


Figure 5: Transverse distribution of photodetached electrons 5 cm downstream of the laser volume.

By modifying the laser waist to 100 μm , the impact of the laser's hyperbolic silhouette can be reduced as the Rayleigh length grows larger than the ion beam transverse beam size. This results in an approximately constant laser radius in the area of interaction. Multiple scans were taken at 2 mm steps in the vertical plane, with a primary beam consisting of a million H^- ions. Sampling the electrons for each laser position 5 cm downstream of the laser allows a beam profile to be constructed from the number of electrons produced

by the interaction as seen in Fig. 6. The fit found the beam size to be $\sigma_y = 3.5 \pm 2.7 \times 10^{-2}$ mm which compared to the input distribution of $\sigma_y = 3.35$ mm is in good agreement.

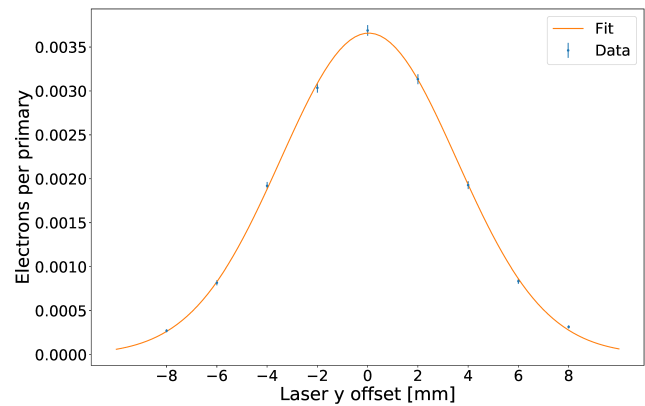


Figure 6: Constructed beam profile produced by scanning the laser across the input H^- beam and counting the ejected electrons in photodetachment process.

SUMMARY AND OUTLOOK

This study presents example simulations of two unique processes recently added to BDSIM: photodetachment for H^- ions and inverse Compton scattering for charged particles. Both processes can be applied to model particle-photon interactions in simulations of laserwire diagnostic experiments. The model creates a laser volume characterised with Gaussian beam optics. A probabilistic approach was used to sample interacted particles from input distributions. In the case of photodetachment the incoming H^- ion is neutralised and a secondary electron is generated. For inverse Compton scattering a secondary photon is generated with correlated energy and beam line axis angle.

The results presented here demonstrate an example energy spectrum of the scattered photons generated in the inverse Compton scattering process. The simulation for the photodetachment process shows the convolution of the Gaussian beam optics of the laser with the particle beam.

ACKNOWLEDGEMENTS

Work supported by UK STFC grants ST/N001753/1, ST/P003028/1 and ST/P00203X/1.

REFERENCES

- [1] S. M. Gibson *et al.*, "Overview of Laserwire Beam Profile and Emittance Measurements for High Power Proton Accelerators", in *Proc. 2nd Int. Beam Instrumentation Conf. (IBIC'13)*, Oxford, UK, Sep. 2013, paper TUPF15, pp. 531–534.
- [2] A. Kurup, J. K. Pozimski, P. Savage, S. M. Gibson, K. O. Kruchinin, and A. P. Letchford, "Simulations of the FETS Laser Diagnostic", in *Proc. 4th Int. Beam Instrumentation Conf. IBIC'15*, Melbourne, Australia, Sep. 2015, pp. 521–525.
- [3] S. Henderson *et al.*, "The Spallation Neutron Source accelerator system design", *Nuclear Instruments and Methods in*

Physics Research Section A: Accelerators, Spectrometers, Detectors and Associated Equipment, vol. 763, pp. 610-673, Nov. 2014.

- [4] T. Hofmann *et al.*, “Demonstration of a laserwire emittance scanner for hydrogen ion beams at CERN”, *Phys. Rev. ST Accel. Beams*, vol. 18, issue 12, p. 122801, Dec. 2015.
- [5] T. Hofmann *et al.*, “Experimental Results of the Laserwire Emittance Scanner for LINAC4 at CERN”, *Nuclear Instruments and Methods in Physics Research Section A: Accelerators, Spectrometers, Detectors and Associated Equipment*, vol. 830, pp. 526-531, Sep. 2016.
- [6] L. J. Nevay *et al.*, “Laserwire at the Accelerator Test Facility 2 with submicrometer resolution”, *Physical Review Special Topics - Accelerators and Beams*, vol. 17, no. 7, p. 072802, July 2014.
- [7] T. Aumeyr *et al.*, “A 2-D Laser-wire Scanner at PETRA-III”, in *Proc. 1st Int. Particle Accelerator Conf. IPAC'10*, Kyoto, Japan, May 2010, paper MOPE069, pp. 1137–1139.
- [8] L. J. Nevay *et al.*, “BDSIM: An Accelerator Tracking Code with Particle-Matter Interactions”, arXiv:1808.10745v1 [physics.comp-ph] 31 Aug. 2018.
- [9] K. O. Kruchinin *et al.*, “Simulation Results of the FETS Laserwire Emittance Scanner”, in *Proc. 5th Int. Particle Accelerator Conf. IPAC'14*, Dresden, Germany, Jun. 2014, pp. 3729–3731.
- [10] T. Hofmann, E. Bravin, U. Raich, F. Roncarolo, and B. Cheymol, “Laser Based Stripping System for Measurement of the Transverse Emittance of H- Beams at the CERN LINAC4”, in *Proc. 4th Int. Particle Accelerator Conf. IPAC'13*, Shanghai, China, May 2013, paper MOPME075, pp. 652–654.
- [11] J. T. Broad and W. P. Reinhardt, “One- and two-electron photoejection from H⁻: A multichannel *J*-matrix calculation”, *Phys. Rev. A*, vol. 14, issue 6, pp. 2159-2173, Dec. 1976.
- [12] O. Klein and Nishina, “On the scattering of radiation by free electrons according to the new relativistic quantum dynamics of Dirac”, *YZ Physics*, vol. 52, p. 853, 1929.

Content from this work may be used under the terms of the CC BY 3.0 licence (© 2019). Any distribution of this work must maintain attribution to the author(s), title of the work, publisher, and DOI